Synthesis and characterization of SnO2: Ti thin films spray-deposited

Demet Tatar, Mehmet Ertuğrul

Abstract— In this study, we have newly developed titanium-tin oxide (TiSnO) thin films as the transparent conducting oxides materials by the spray pyrolysis technique. Tin oxide thin films doped with different Ti content were successfully grown by spray pyrolysis and they were characterized as a function of Ti content. The effect of Ti contents on the crystalline structure and optical properties of the as-deposited SnO2:Ti films was systematically investigated by X-ray diffraction (XRD), scanning electronic microscopy (SEM) and UV-vis spectrometer. The X-ray diffraction patterns taken at room temperature showed that the films are polycrystalline. The preferred directions of crystal growth appeared in the difractogram of SnO2: Ti (TiTO) films were correspond to the reflections from the (110), (200), (211) and (301) planes. The grain size varies from 21.802 to 27.863 nm, respectively. SEM study reveals the surface of TiTO to be made of nanocrystalline particles. The highest visible transmittance (570 nm) of the deposited films is 80 % for 20 wt % titanium doped tin oxide films. The obtained results revealed that the structures and optical properties of the films were greatly affected by doping levels. These films are useful as conducting layers in electro chromic and photovoltaic devices.

Index Terms— Transparent conducting oxide, SnO2: Ti; optoelectronic; gas sensor, spray pyrolysis;

I. INTRODUCTION

The highly transparent and conductive thin films, owing to its high transmittance and conductivity, have been wide device applications [1, 2]. In recently years there has been a growing interest in the use of transparent conducting oxide thin films as conducting solar window materials in thin film solar cells [3, 4, 5, 6], heat reflectors for advanced glazing in solar application [7, 8] and as various gas sensors [5-13]. Tin oxide is the first transparent conductor to have received significant commercialization [5, 9, 14]. SnO_2 is chemically inert, mechanically hard, and can resist high temperature [5]. Many excellent reviews of transparent conductive oxides are available [15]. SnO_2 either doped or undoped can be synthesized by numerous techniques such as thermal evaporation [3, 9], sputtering [5, 9-12, 16, 17], chemical vapour deposition [3, 18-20], sol-gel dip coating [3, 17, 21], painting [3, 17, 22], spray pyrolysis [3, 5, 7, 13, 20, 23-26], hydrothermal method [27] and pyrosol deposition [3, 20, 28-30]. Among the various deposition techniques, the spray pyrolysis is the well suited for the preparation of doped tin oxide thin films because of its simple and inexpensive experimental arrangement, ease of adding various doping material, reproducibility, high growth rate, and mass

Demet Tatar, Pasinler MYO, Department of Electronic, Ataturk University, Erzurum 25240, Turkey

Mehmet Ertuğrul, Engineering Faculty, Department of Electric and Electronic Engineering, Ataturk University, Erzurum 25240, Turkey

production capability for uniform large area coatings, which are desirable for industrial solar cell applications [3, 5, 11, 13, 17, 23, 31, 32]. However, economical large area film production is the essential characteristic of the simple spray pyrolysis technique [16].

Therefore, there is a considerable interest in understanding the microstructure and optical properties of doped SnO films, which will give more chance for potential applications. The doping elements can also improve microstructural, morphological and mechanical features of SnO_2. At present, a number of SnO films doped with various metallic ions have been widely studied for the manipulation of their optical and electrical properties, Such as F, Sb, Nb, Mo, W and V. But, firstly in this study, SnO_2 structure have been doping with Ti element as alternative cation and their effect on SnO_2 have been investigated.

II. EXPERIMENTAL DETAILS

The titanium doped tin oxide thin films reported in the present study were prepared using a homemade spray pyrolysis apparatus. Thin films of SnO_2: Ti (TiTO) were deposited on optical glass substrate (75x25x1 mm^3). Dehydrate stannous chloride ($SnCl_2.2H_2O$ with 98% purity, Merck) was used in making the precursor solution for SnO_2 thin films. 10 g of $SnCl_2.2H_2O$ dissolved in 5 ml of concentrated hydrochloric acid (HCl) was heated at 90 °C for 10 min. The addition of HCl was required in order to break down the polymer molecules that were formed when diluting with methanol. This mixture was diluted by adding methanol served as starting solution and the diluted solution was made up to 25 ml. For titanium doping, titanium (IV) isopropxide (with 97% purity, Aldrich) dissolved in etonol (25 ml) was added to the starting solution, in such a way as to result in titanium doping in the range of 1,5,10,15,20 and 25wt %. In each case, the amount of spray solutions prepared was 50 ml. All the spray solutions were magnetically stirred for 1h and finally these solutions were filtered by syringe filter with 0.2 µm pore size before spraying on substrate. The microscopic glasses with 75x25x1 mm^3 dimesions were used as substrates. The substrates were washed with water, then boiled in concentrated chromic acid and kept in distilled water for 48 h [4]; finally substrates were cleaned with organic solvents and helping ultrasonic cleaner. The substrates were pre-heated to the required temperature. The normalized distance between the spray nozzle and the substrate is 40 cm the spray angle (α) is 45°. The flow rate (1.25 ml/min.), total spraying quantity (50 ml) and plate rotation speed (20 rpm/min.) were all kept fixed. Filtered compressed air was used as carrier gas. The flow rate of air used as a carrier gas is about 1.25 ml/min. The total deposition time was maintained at 40 minutes for each

film. The substrate temperature (working temperature) was 440 °C. The substrate temperature was maintained using a k-type thermocouple based digital temperature controller. Uniform coating was achieved by rotating the substrate with a speed of 20 rpm/min in its plane. The samples were produced simultaneously at substrate temperature 440 °C. After deposition, the coated substrates were allowed to cool down naturally to room temperature. In each process, more ten samples were produced simultaneously at each doping levels. It was realized that the crystals have similar properties and then passed to other processes.

The structural characterization of the films was carried out by X-ray diffraction (XRD) measurements using a Rigaku D/Max-IIIC diffractometer with CuKα radiation (λ=1.5418 Å), at 30 kV, 10 mA. Film thickness was measured by a conventional mass method and were confirmed with the Swanepoel method[30, 36]. Surface morphology of the resulting films was scanning electrom microscopy (SEM), which was produced by FEI inspect S50 SEM, respectively. Optical transmittance measurements of the FTO films were measured using UV-Vis spectrophotometer (Perkin Elmer, Lambda 35) in the wavelength ranging from 300 to 1000 nm.

III. RESULTS AND DISCUSSION

3.1. Structural properties

The microstructural characterization of the films are made with X-ray diffraction spectra (XRD). Fig. 1 shows the XRD curves of undoped and Ti doped SnO_2 thin films. It is seen that all peaks belong to SnO_2 tetragonal cassiterite structure (JCPDS 41-1445). The films are polycrystalline and two directions of crystal growth appeared in the difractogram of the film deposited at the lower doping concentration, which correspond to the reflections from the (110) and (200) planes. With the increase in the doping concentration a new direction of crystal growth appeared, which corresponds to the reflection from the (211) and (301) plane. The presence of other peaks such as (101), (220) and (310) have also been detected but with substantially lower intensities at the higher doping concentration, which means the crystal growth was enhanced and the grain size had increased. The films grow along (110) preferred orientation and secondary most striking peak is (211), irrespective of Ti doping. The peaks of (101),

(200), (220), (310) and (301) are also observed from Fig. 1. The peak intensities of undoped film slightly increase with Ti doping ratio till 5 at.% Ti level and then it decrease gradually with more Ti doping.
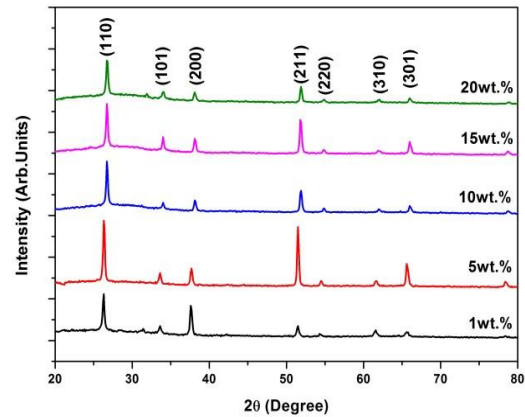

Fig. 1. *XRD spectra of the SnO₂:Ti films deposited on glass at different concentration*

The lattice constant a and c, for the tetragonal phase structure is determined by the relation $(1/d^2)=\{[(h^2+k^2)/a^2]+(l^2/c^2)\}$ where d is the inter planer distance and (hkl) are miller indices, respectively. The calculated lattice constant a and c were given in Table 1. The lattice parameters 'a' and 'c' are found to vary from 4. 795 to 4. 722 and 3.209 and 3.179 Å for 'a' and 'c', respectively. The change in lattice constant for the spray-deposited thin film over the bulk clearly suggested that the film grains are strained, which may be due to the nature and concentration of the native imperfections changing[33].

The grain size of TiTO films deposited with different doping levels is calculated using Scherrer's Formula [4, 20, 26, 31], $D=0.9\lambda/(\beta cos\theta)$, the dislocation density (δ) values of films are calculated by $\delta=1/D^2$ and the microstrain (ε) values of films are determined by $\varepsilon=(1/sin\theta)[(\lambda/D)-(\beta cos\theta)]$, where D is the size of crystallite, β is the broadening of diffraction line measured at half its maximum intensity in radians and λ is wavelength of X-rays (λ=1.5418 Å). The calculated grain size, dislocation density and microstrain values are given in Table 1.

The grain size of 25.014 nm for 1 wt.% Ti sample start to increase as soon as Ti element entrance to SnO_2 structure and it reaches to maximum value of 27.863 nm for 5 wt.% Ti

Sample	(hkl)	dst (Å)	dobs (Å)	a (Å)	c (Å)	D (nm)	δx10¹¹ lines/cm²	εx10⁻⁴
	110	3,347	3,389			25,014	1,598	27,1
	101	2,643	2,667			12,259	6,654	43,5
	200	2,369	2,392			25,249	1,568	18,9
1wt.%	211	1,764	1,774	4.795	3.203	23,489	1,813	15,1
	220	1,675	1,689			15,848	3,982	21,3
	310	1,498	1,506			16,272	3,777	18,5
	301	1,416	1,423			16,098	3,859	17,7
								9,4
	321	1,215	1,219			25,942	1,486	

	(hkl)							
	110	3,347	3,389			27,863	1,288	24,3
	101	2,643	2,667			19,668	2,585	27,1
	200	2,369	2,386			25,612	1,524	18,6
	211	1,764	1,774	4,793	3,209	31,234	1,025	11,4
5wt.%	220	1,675	1,684			21,003	2,267	16
	310	1,498	1,503			19,232	2,703	15,6
	301	1,416	1,423			25,859	1,495	11
	321	1,215	1,219			23,512	1,809	10,4
	110	3,347	3,339			26,533	1,420	25,2
	101	2,643	2,637			8,540	13,711	61,7
	200	2,369	2,362			20,346	2,416	23,2
	211	1,764	1,762	4,722	3,179	25,744	1,509	13,7
10wt.%	220	1,675	1,672			17,869	3,132	18,7
	310	1,498	1,497			16,929	3,489	17,7
	301	1,416	1,415			22,003	2,065	12,9
	321	1,215	1,215			18,824	2,822	12,9
	110	3,347	3,339			25,456	1,543	26,2
	101	2,643	2,637			24,005	1,735	22
	200	2,369	2,362			21,062	2,254	22,4
15wt.%	211	1,764	1,765	4,722	3,179	27,390	1,333	12,9
	220	1,675	1,675			18,606	2,889	18
	310	1,498	1,499			13,667	5,354	21,9
	301	1,416	1,415			23,381	1,829	12,1
	321	1,215	1,216			22,629	1,953	10,7
	110	3,347	3,339			21,802	2,104	30,6
	101	2,643	2,637			9,338	11,467	56,5
	200	2,369	2,362			17,470	3,276	27
20wt.%	211	1,764	1,762	4,722	3,179	26,400	1,435	13,3
	220	1,675	1,672			12,552	6,347	26,6
	310	1,498	1,495			14,710	4,621	20,3
	301	1,416	1,415			20,382	2,407	13,9
	321	1,215	1,212			25,748	1,508	9,414

Table 1. *Structural parameters table of the SnO_2:Ti films at different concentration*

[Standard JCPDS card no:41-1445; a=4.738 c=3.187, Standard and calculated for 'd' values. the size of crystallite (D), the dislocation density (δ) and the microstrain(ε)] imperfect in a crystal associated with the mis-registry of the lattice in one part of the crystal with respect to another part. Unlike, vacancies and interstitials atoms, dislocations are insufficient to account for their existence in the observed dislocation densities [34, 35, 36]. The dislocation density and microstrain values of 1.598×10^{11} lines/cm² and 27.1×10^{-4} for 1 wt.% Ti doped SnO_2 decrease gradually to minimum values of 1.288×10^{11} lines/cm² and 24.3×10^{-4} with Ti content till 5 at.% level. When Ti doping ratio is increased over 10 at.% content, they begin to increase. Because the low values of dislocation density and microstrain indicate lower geometric mismatches and defects, the best crystalline properties are observed for 5 at.% Ti doped SnO_2, which can be also seen from XRD peak intensities.
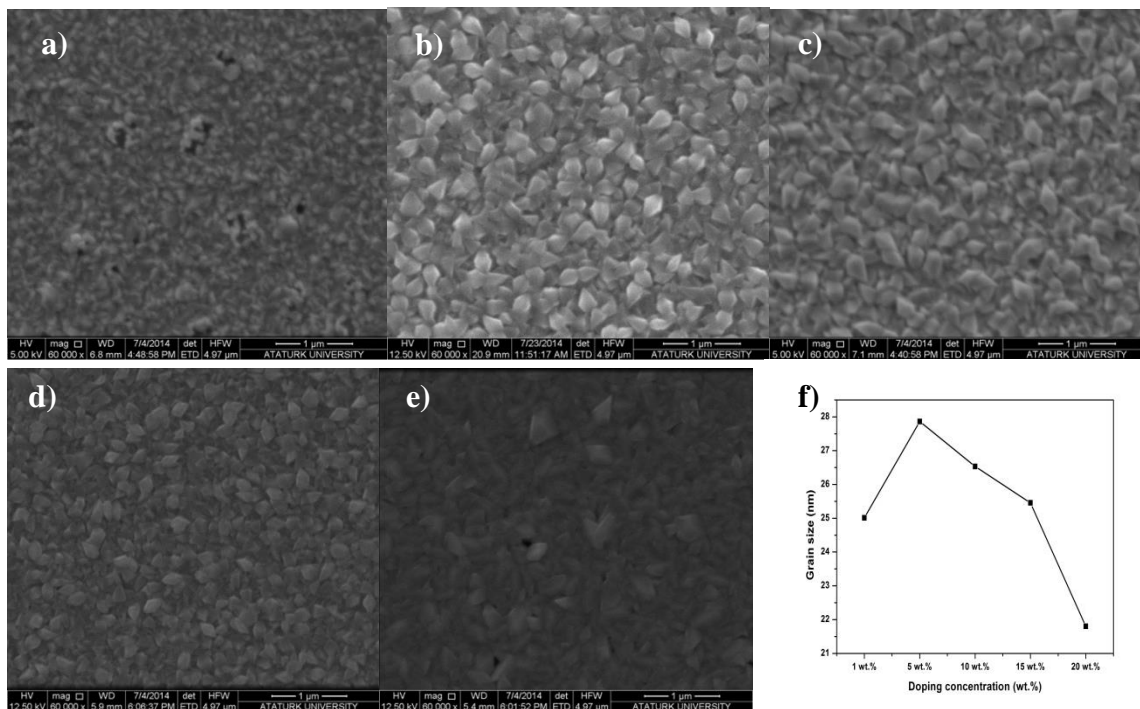
Fig. 2. SEM micrographs SnO_2:Ti films obtained for different deposition concentration [(a)1wt.%, (b) 5 wt. %, (c) 10 wt. %, (d) 15wt. %, (e) 20 wt. %, respectively and (f) Grain size of various deposition concentration in SnO2:Ti films]

The surface morphology of Ti doped SnO_2 films were investigated by SEM micrographs and are shown in Fig. 2. It is observed that the surface morphology of the films depends on Ti doping concentration. It can be seen that the films are made up of grains with pyramidal and polyhedron like shape. Also, smaller and more slender grains were seen mostly in the spaces between the larger needle shaped grains which characterize the films. It can be concluded from XRD analyses and SEM observations that bigger and faceting grains probably indicate (110) orientation and; smaller and needle shaped grains belong to (211) orientations. As the Ti doping concentration increased to 5 at.%, grains continuously become bigger and again their sizes decrease for further Ti doping. As the Ti doping concentration increased to 5 at.%, the number of smaller grains increases, but, for 10 and 15 at.% Ti doped samples, these grains enlarge and the number of smaller grains decreases. For the 20 at.% Ti doped sample, the polyhedron like grains again dwindle and the number of grains increases (decrease in the grain sizes). Ti doped SnO_2 films has very homogenously dispersed well-formed nanoparticle structure and this homogeneity increases with further Ti doping. The films particle structure begins to be more prominent with 5 at.% Ti doping ratio. The grain size variation with Ti doping being seen from SEM images corroborates the XRD results. The grains on the layers are randomly grown and giving a rise in scattering effect, thereby reducing transmittance.

3.3. Optical properties

Optical properties of Ti doped SnO_2 thin films have been investigated by UV–VIS spectrometer at room temperature. Fig.3 shows the variation of transmittance (T) with respect to wavelength of TiTO thin films with different titanium doping levels. The transmittance of 20 wt% Ti concentration is maximum; it is 80% (570nm), (Table.1). The increase in transmittance is attributed to both the well-crystallized film and the pinhole free surface [30]. The transmittance spectra obtained from the deposited films are comparatively shown in Fig. 4 as a function of the Ti doping levels. The average visible (400–800 nm). From the transmittance curves, it is seen that the transmittance of film is strongly affected by the Ti doping concentration and the transmittance of all samples increase with increasing wavelength. It is observed that transmittance shows increasing tendency with Ti doping concentration.
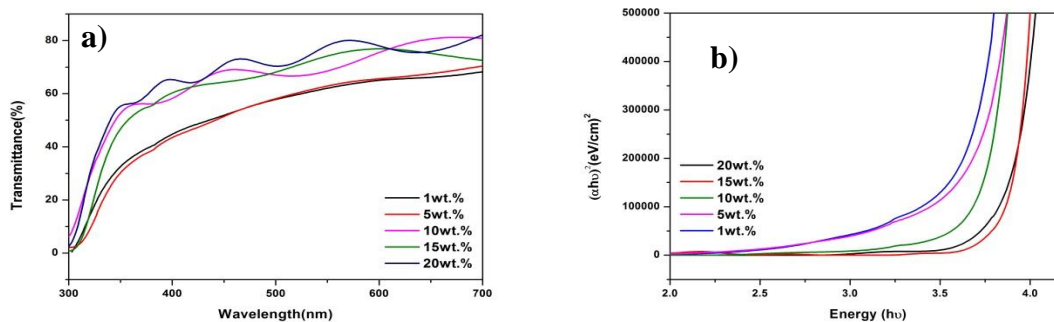
Fig. 3. a) Optical transmission spectra and b) $(\alpha h\nu)^2$ vs. (hv) curves of SnO_2:Ti thin films as a function of Ti-doping concentration

The optical bandgap (Eg) was estimated from the extrapolation of linear portion in the plot of absorption coefficient (α2) versus photon energy (hv) [37].

E_g values are determined by plotting $(\alpha h\upsilon)^2$ vs. $h\upsilon$ and extrapolating of the linear region of the plot to zero absorption $((\alpha h\upsilon)^2 = 0)$. It is clearly seen in Fig. 3b that the band gap values increase with an increase of Ti content in the SnO_2 structures. The Eg is found to increase with the increasing Ti doping levels, which is ranging between ~3.51 and 3.87 eV. The band gap values of 1.0, 5.0, 10.0, 15.0 and 20.0 at.% Ti doped SnO_2 thin films are found as 3.51 eV, 3.57 eV, 3.68 eV, 3.87 eV and 3.85 eV, respectively.

IV. CONCLUSIONS

Polycrytalline thin films of SnO_2 with different ([Ti]/[Sn] ratios) titanium doping concentrations were prepared using a homemade spray pyrolysis apparatus at substrate temperatures 400 ºC on to optical glasses. The effects of doping levels on SnO_2: Ti films structural and optical properties were experimentally investigated. X-ray diffraction studies reveal that the material in the thin form is polycrystalline with tetragonal structure. The XRD studies confirmed the polycrystalline tetragonal tin oxide (TO) structure. It is perceptible that the intensity of the (110) diffraction peak obtained from 1 at.% Ti doped films is slightly higher than that of the (211) peak, thus indicating a slight preferential growth along the (110) direction for the growth condition adopted in this work. The data extracted from the XRD analysis are summarized in Table. 1. The effect of Ti doping on morphological properties of SnO_2 are investigated by SEM micrographs, which is given in Fig. 2. Ti doped SnO_2 films has very homogenously dispersed well-formed nanoparticle structure and this homogeneity increases with further Ti doping. The bigger pyramidal and smaller polyhedron shaped grains are dominant grain structures in the films, which probably indicates (110) and (211) XRD planes. The grain sizes of undoped film increase with increasing Ti doping ratio up to 5 at.% Ti doping ratio and then it starts to decrease with more Ti content. The grain size variations with doping ratio is a good agreement with XRD results.

In this study, we have newly developed titanium-tin oxide (TiSnO) thin films as the transparent conducting oxides materials by the spray pyrolysis technique. Tin oxide thin films doped with different Ti content were successfully grown by spray pyrolysis and they were characterized as a function of Ti content. Firstly in this study, SnO_2 structure have been doping with Ti element as alternative cation and their effect on SnO_2 have been investigated.

REFERENCES

[1] D. Miao, Q. Zhaoa, S. Wua, Z. Wange, X. Zihanga and X. Zhaoa, Journal of Non-Crystalline Solids 356, 2557 (2010).

[2] J. Gregory, Exarhos and Xiao Dong, Zhou, Thin Solid Films 515, 7025 (2007).

[3] E. Elengovan, K.Ramamurthi, Journal of Optoelectronics and Advanced Materials 5/1, 45 (2003).

[4] A. A. Yadava, E.U. Masumdara, A.V. Moholkar, M. Neumann-Spallartc, K.Y. Rajpured and C.H. Bhosaled, Journal of Alloys and Compounds 448, 350 (2009).

[5] B. Thangaraju, Thin Solid Films 402, 71 (2002).

[6] A. Goetzberger, C. Hebling, Sol. Energy Mater. Sol. Cells 62, 1 (2000).

[7] G. Frank, E. Kaur, H. Kostlin, Sol. Energy Mater. 8, 387 (1983).

[8] S. Chen, Thin Solid Films; 77, 127 (1981).

[9] W.Y. Chung, C.H. Shim, S.D. Choi, D.D. Lee, Sens. Act. B 20, 139 (1994).

[10] J. R. Brown, P. W. Haycock, L. M. Smith, A. C Jones, E. W. Williams, Sens. Act. B 63, 109 (2000).

[11] P. Nelli, G. Faglia, G. Sbeveglieri, E. Cerede, G. Gabetta, A. Dieguez, J. R. Morante, Thin Solid Films 371, 249 (2000).

[12] I. Stambolova, K. Konstantinov, T. Tsacheva, Mater. Cham Phys. 63, 177 (2000).

[13] S.U. Lee, W.S. Choi and B. Hong, Phys.Scr. T. 129, 312 (2007).

[14] E. Elangovan, S. A. Shivashankar, K. Ramamurthi, Journal of Crystal Growth 276, 215 (2005).

[15] P. S. Patil, Mater. Chem. Phys. 59, 185 (1999).

[16] M. Ruske, G. Brauer, Szczrbowski J, Thin Solid Films 351, 146 (1999).

[17] Q. Zhao, S. Wu, D. Miao, Advanced Materials Research, 150-151, 1043 (2011).

[18] D. Belanger, J.P. Dotelet, B.A. Lombos, J. I. Dickson, J. Electrochem Soc. 398, 1321 (1985).

[19] A. C. Arias, L. S. Roman, T. Kugler, R. Toniola, M.S. Meruvia, I. A. Hummelgen, Thin Solid Films 371, 201 (2000).

[20] P.S. Shewale, S. I. Patil, M. D. Uplane, Semicond. Sci. Technol. 25, 115008 (2010).

[21] O.K. Varghese, L.K. Malhotra, J.Appl.Phys. 87, 7457 (2000).

[22] M.K. Karanjai, D.D. Gupta, J. Phys. D: Appl. Phys. 21, 356 (1988).

[23] G. Gordillo, L.C. Moreno, W.de la Cruz, P. Theran, Thin Solid Films 252, 61 (1994).

[24] A. Malik, A. Seco, E. Fortunato, R. Martin, J. Non-Cryst. Solids 1092, 227 (1998).

[25] B. Zhang, Y. Tian, J.C. Zhang and W. Cai, J. Mater Sci. 46, 1884 (2011).

[26] A.V. Moholkara, S. M. Pawara, K. Y. Rajpureb, S. N. Almaric, P. S. Patilb and C. H. Bhosale, Solar Energy Materials and Solar Cells, 92, 1439 (2008).

[27] Q. Chen, Y. Qian, Z. Chen, G. Zhou, Y. Zhang, Thin Solid Films 264, 25 (1995).

[28] A. Smith, J. M. Laurent, D. S. Smith, J. P. Bonnet, R.R. Clemente, Thin Solid Films 266, 20 (1995).

[29] K. Omura, P. Veluchamy, M. Murozono, J. Elecktrochem. Soc. 146, 2113 (1999).

[30] A.V. Moholkar, S.M. Pawara, K.Y. Rajpure, C.H. Bhosale, J.H. Kim, Applied Surface Science 255, 9358 (2009).

[31] N. Menarian, S.M. Rozati, E. Elemurugu, E. Fortunato, Phys. Status Solidi C 79, 2277 (2010).

[32] E. Elengovan, K. Ramamurthi, Applied Surface Science, 249, 183 (2005).

[33] C.M.Shen, X.G.Zhang, H.L.Ll., Appl. Surf. Sci. 240, 34 (2005).

[34] R.R. Kasar, N. G. Deshpande, Y. G. Gudage, J. C. Vyas, R. Sharma, Physica B 403, 3724 (2008).

[35] A. Beltron, J. Andres, Appl.Phys.Lett. 83, 635 (2003).

[36] M.Bedir, M.Öztaş,O.F.Bakkaloglu, R.Ormanel, Eur.Phys.J.B. 45, 465 (2005).

[37] I. Hamberg, C.G. Granqvist, J. Appl. Phys. 60 (1986) R123